# Swiss Similarity Studies of 5,7-dihydroxy-2-(4-hydroxyphenyl) chromen-4-one: A Promising Role against Sickle cell disease

**Yemisi Elizabeth ASIBOR[1], Nathaniel Oladoye OLATUNJI[3], Dayo Felix LATONA[1], Abel Kolawole OYEBAMIJI [2], and Banjo SEMIRE [3*]**

[1] Osun State University, Department of Pure and Applied Chemistry, Osogbo, Nigeria.
[2]Bowen University, Department of Chemistry and Industrial Chemistry, Iwo, Osun State, Nigeria.
[3] Computational Chemistry Laboratory, Department of Pure and Applied Chemistry, Ladoke Akintola University of Technology, Ogbomoso, Oyo State, Nigeria.
Corresponding email: bsemire@lautech.edu.ng
DOI: 10.56201/ijhpr.vol.10.no1.2025.pg43.63

***Abstract***
*Swiss Similarity Studies were carried out on 5,7-dihydroxy-2-(4-hydroxyphenyl)chromen-4-one (A28) to estimate the anti-sickle properties of the compound. Seven compounds similar to 5,7-dihydroxy-2-(4-hydroxyphenyl)chromen-4-one were obtained, A28-1, A28-2, A28-3, A28-4, A28-5, A28-6 and A28-7. The Swiss ADMET and Pro-tox II tools were utilized for ADMET profiling of these compounds. Six compounds with good ADMET properties and conventional drug (Rivaroxaban) were optimized at DFT, docked with (PBD: 5E6E, 6DI4, and 6WBU). Molecular docking analysis showed that A28-2 and A28-4 had -9.1 kcal/mol and -9.2 kcal/mol binding affinities with 5E6E, A28-3 -8.7 kcal/mol had binding affinity with 6D14, A28-2 and A28-4 had binding affinities -9.5 kcal/mol and -9.9 kcal/mol binding affinities with 6BWU. Rivaroxaban had -8.5 kcal/mol, -8.0 kcal/mol, and -8.1 kcal/mol binding affinities with 5E6E, 6D14, and 6BWU respectively. From the docking results, compounds A28-2, A28-3, and A28-4 show a stronger therapeutic potential than rivaroxaban.*
***Keywords:*** *ADMET, DFT, Molecular docking, Sickle Cell Diseases, Swiss Similarity*

## 1.0 Introduction

Sickle cell disease is one of the most common inherited blood disorders globally, affecting millions of individuals, particularly those of African, Mediterranean, Middle Eastern, and Indian descent (Serjeant, 2010). The pathophysiology of SCD stems from a single nucleotide mutation (GAG → GTG) in the sixth codon of the β-globin gene, resulting in the substitution of valine for glutamic acid in the hemoglobin molecule (Piel et al., 2017, Rees et al., 2010). This seemingly minor alteration has profound consequences on hemoglobin's behavior, leading to the polymerization of HbS when deoxygenated, which in turn causes red blood cell sickling. The rigid, crescent-shaped cells have reduced deformability, leading to vaso-occlusion and chronic hemolysis, hallmark features of the disease.

Standard treatments, including hydroxyurea and transfusion therapy, have demonstrated efficacy in reducing the frequency of painful crises and improving quality of life. However, they are not curative, and their long-term use may result in complications such as iron overload,

cytotoxicity, or limited efficacy in certain populations (Ware et al., 2017). Advances in gene therapy offer hope for a potential cure, but high costs and complex delivery methods limit their feasibility in low-income regions, where the majority of patients reside. This underscores the necessity of developing novel, cost-effective treatments that target the underlying mechanisms of SCD.

Natural compounds have gained significant attention in the search for novel therapeutic agents. In recent years, naturally derived compounds have attracted significant interest for their potential in treating various diseases, including SCD. Flavonoids, a class of polyphenolic compounds found in plants, have long been recognized for their therapeutic potential in various diseases due to their diverse biological activities. These include antioxidant, anti-inflammatory, and hemoglobin-modifying properties (Middleton *et al.*, 2000). These compounds are abundant in fruits, vegetables, and medicinal plants and have been shown to exert anti-inflammatory, antioxidant, and anti-hemolytic effects (*Middleton et al.*, 2000). Computational screening of some Nigeria medicinal plants using PASS, DFT, SwissADMET, ADMETSar 2.0, molecular docking and molecular dynamic simulations in the management of sickle cel disease, twenty-six (26) potential compounds for managing sickle cell disease were evaluated for their drug-likeness in treating sickle cell disease (Asibor *et al.*, 2024). In the context of SCD, flavonoids' antioxidant properties are particularly significant, as oxidative stress plays a key role in the pathogenesis of the disease. Elevated levels of reactive oxygen species (ROS) contribute to the polymerization of HbS, hemolysis, and endothelial dysfunction, exacerbating disease severity (Nur *et al.*, 2011). Among the flavonoids, 5,7-dihydroxy-2-(4-hydroxyphenyl)chrome-4-one stands out due to its structural and functional attributes. Preliminary studies suggest that this compound can stabilize hemoglobin's native conformation, potentially reducing HbS polymerization and subsequent sickling (Pérez *et al.*, 2024). Furthermore, its ability to scavenge ROS and modulate oxidative pathways offers additional therapeutic benefits. Exploring its analogs through computational screening may uncover structurally similar molecules with enhanced efficacy and bioavailability. Among these, flavonoids, a class of polyphenolic compounds found in plants, have demonstrated a wide range of biological activities. These include antioxidant, anti-inflammatory, and hemoglobin-modifying properties (Middleton *et al.*, 2000). One promising flavonoid, 5,7-dihydroxy-2-(4-hydroxyphenyl)chrome-4-one, exhibits a unique chemical structure that suggests potential for stabilizing hemoglobin and mitigating HbS polymerization. This compound's ability to modulate oxidative stress and its affinity for hemoglobin has positioned it as a candidate for further investigation in the context of SCD.

Swisssimilarity is a web-based virtual screening tool that leverages ligand-based and structure-based approaches to identify compounds with molecular similarity to a reference molecule (Zoete et al., 2016). This computational technique provides insights into potential pharmacological activities, ADMET (absorption, distribution, metabolism, excretion, and toxicity) profiles, and drug-likeness, making it a valuable resource in early-stage drug discovery. The current study leverages Swisssimilarity to evaluate 5,7-dihydroxy-2-(4-hydroxyphenyl)chrome-4-one (an Apigenin) as a potential anti-sickling agent. By integrating computational predictions, this research aims to advance the understanding of flavonoids' role in mitigating sickling and oxidative stress in SCD. The findings could pave the way for the

development of accessible and effective treatments, addressing a critical unmet need in global health care.

## 2.0 Materials and Methods

### 2.1 Swiss Similarity and ADMET Studies

Structure-similar compounds to 5,7-dihydroxy-2-(4-hydroxyphenyl)chromen-4-one were scouted for using the SwissSimilarity platform (http://www.swisssimilarity.ch). The identification of similar compounds aids in predicting potential bioactivity and discovering new therapeutic candidates against sickle cell disease (Bragina *et al.,* 2021). This was done using FP2 fingerprints and pharmacophore screening methods (Zoete *et al.,* 2016). The compounds derived from FP2 fingerprints and pharmacophore screening methods were subjected to Absorption, Distribution, Metabolism, Excretion and Toxicity (ADMET) and Prediction Toxicity of chemical compounds using Pro-Tox II software (Daina and Zoete, 2017: Banerjee *et al.,* 2018). DFT calculations were used to evaluate the molecular descriptors of these similar compounds, using Becke's three parameter hybrid functional with correlation of Lee, Yang, and Parr (B3LYP) (Becke 1993, Lee et al., 1988). The optimization was carried out using the 6-31+G(d,p) basis set in Spartan 14 quantum chemistry software (Jacquemin *et al.,* 2008).

### 2.2 Preparation of the ligands

Similar ligands (A28-1 to A28-6) with high probability, low toxicity, and good ADMET properties were tested against three proteins: hemoglobin S carbonmonoxy sickle hemoglobin (PDB ID: 5E6E, resolution 1.76Å), carboxyhemoglobin (PDB ID: 6BWU, resolution 2.00Å), and destabilize sickle hemoglobin polymer formation (PDB ID: 6DI4, resolution 1.90Å). Rivaroxaban was used as a standard treatment for sickle cell disease. All ligands and the standard drug's 3D SDF conformer were obtained from the PubChem Database (https://pubchem.ncbi.nlm.nih.gov).

### 2.3 Preparation of target protein

The crystal structures of the protein carbonmonoxy sickle hemoglobin with resolution of 1.76Å (PDB ID: 5E6E), Carboxyhemoglobin, PDB ID: 6BWU with resolution of 2.00 Å and destabilize sickle hemoglobin polymer formation PDB ID: 6DI4 with resolution of 1.90 Å were downloaded in PDB format from the protein data bank (http://www.rcsb.org/pdb), Figure 1a, Figure 2d, and Figure 3f. All water molecules, heteroatoms and unwanted complexes were removed from the crystal structure of the downloaded proteins; this was done to ensure that undesired molecular interactions and impurities are avoided, and that no molecules interfered with the potential binding sites of the target proteins during molecular docking. This was done using Discovery Studio Software v.2020 (Shravani *et al.,* 2021; Adepoju *et al.,* 2022). The Ramachandran plot revealed that the receptor was of good quality by using the Volume, Area, Dihedral Angle Reporter (VADAR) (Laskowski and Thornton, 2022) webserver as shown in Figure 1b, Figure 2c, and Figure 3e.

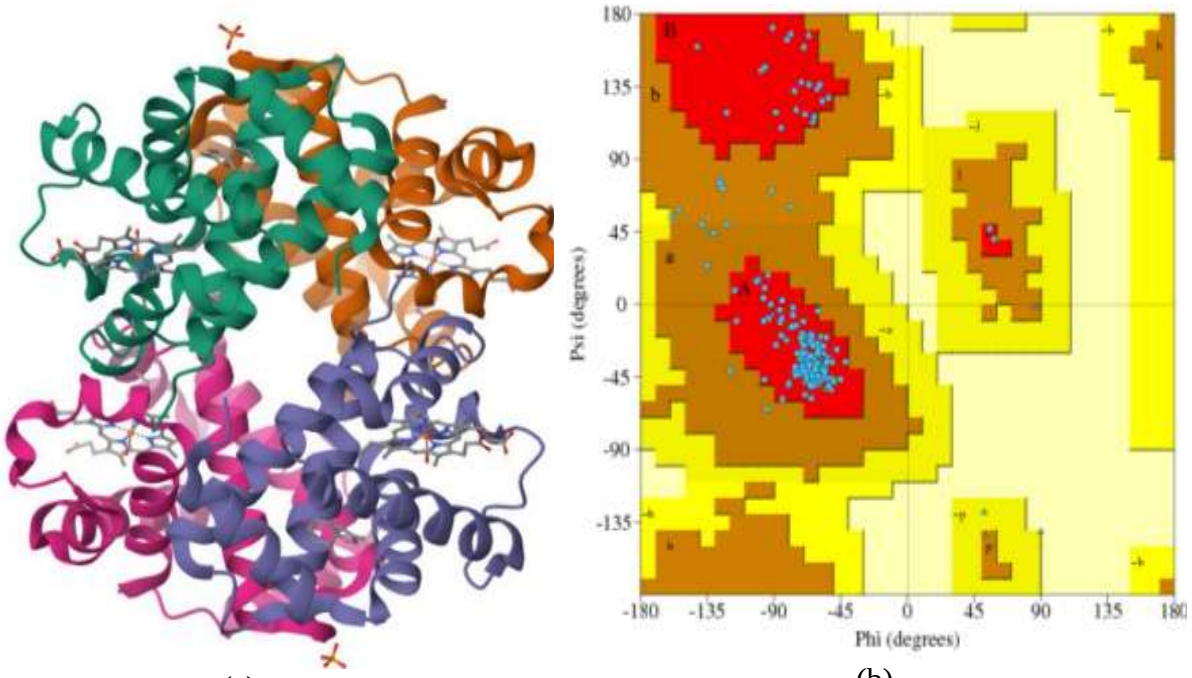


(a) (b)

Figure 1: (a) crystal structure and binding pocket of Carbonmonoxy Sickle Hemoglobin in R-State Conformation (PDB ID: 5E6E) and (b) Ramachandran plot.

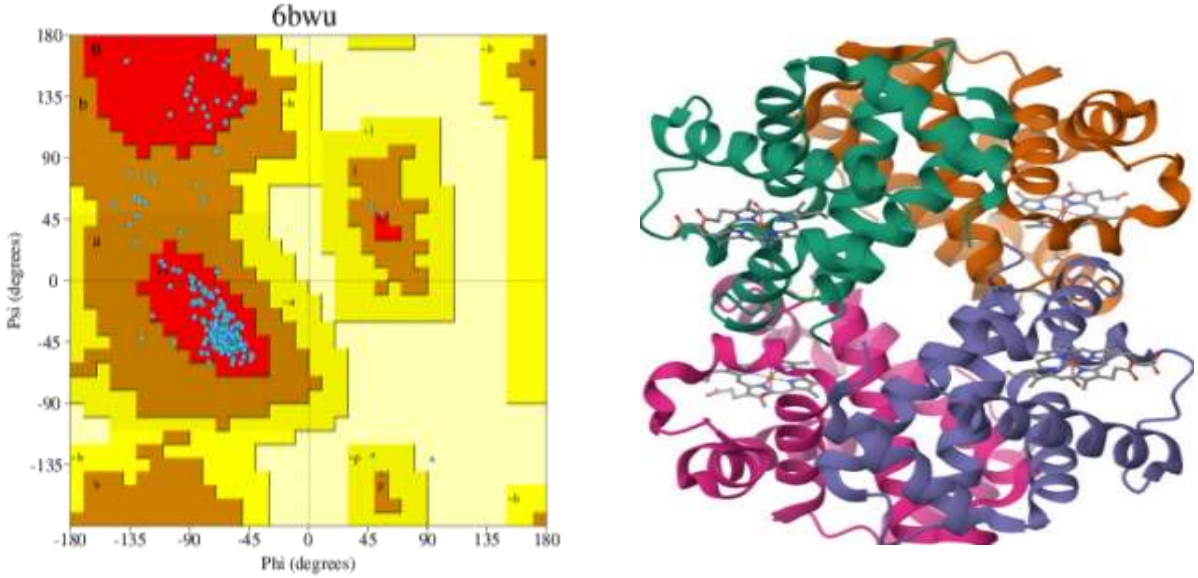


(c) (d)

Figure 2: (c) The crystal structure and binding pocket of carboxyhemoglobin (PDB ID: 6BWU) and (d) Ramachandran plot

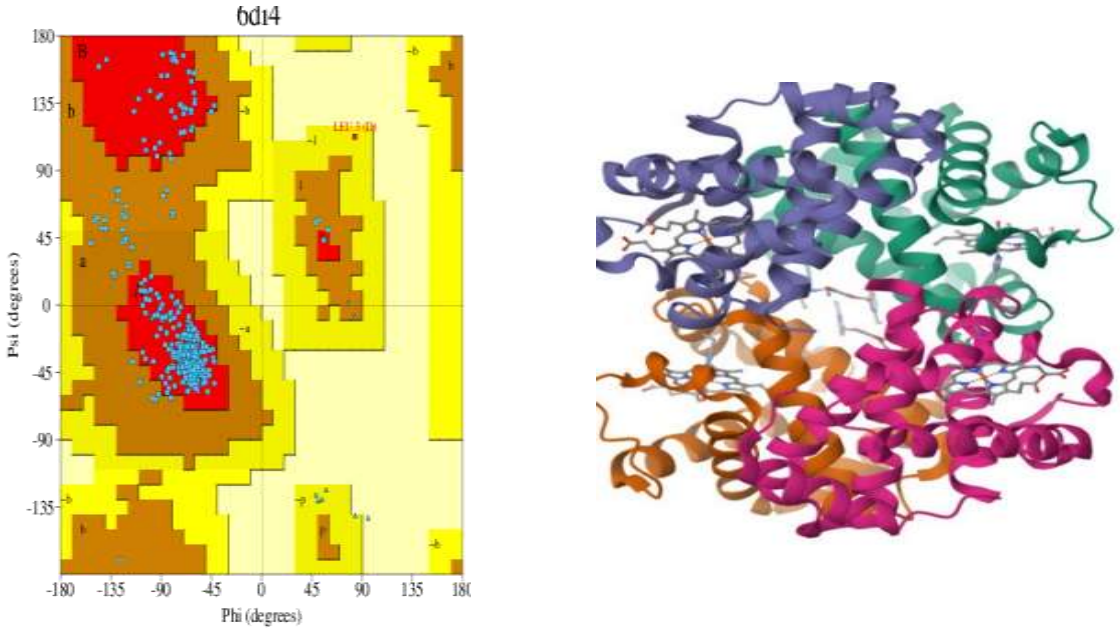


(e) (f)

Figure 3:(e) The crystal structure and binding pocket of destabilize sickle hemoglobin polymer formation (PDB ID: 6DI4) (https://www.rcsb.org/structure/6D14) (f) Ramachandran plot, (PDBsum. www.ebi.ac.uk)

**2.4 Structural and active site analysis of (PDB ID: 5E6E, 6BWU, and 6D14).**

The Computed Atlas for Surface Topography of Proteins (CASTp) (http://sts.bioe.uic.edu/castp /index.html? 2011) (Tian *et al.*, 2018) and Biovia Discovery Studio (2019) were used to identify the binding pockets and amino acid residues in the active sites of carbonmonoxy sickle hemoglobin (PDB ID: 5E6E), carboxyhemoglobin (PDB ID: 6BWU), and destabilize sickle hemoglobin polymer formation (PDB ID: 6DI4). A = 53.352 Å, b = 53.352 Å, and c = 191.068 Å are the crystal dimensions for 5E6E, with angles α (90.00), β (90.00), and ϒ (90.00). The R – values (free and work) are 0.243 and 0.193 while the total accessible surface area (TASA) on the protein is 432.6 Å, 5E6E contains eighty-seven percentage (87%) of the amino acids are in the most favorable region, eleven percentage (11%) are in the unfavorable region and two percentage (2%) of the amino acids are disallowed or forbidden.

The protein carboxyhemoglobin (PDB ID: 6BWU) has a crystal structure with a ninety-one percent (91.8%) favorable region, eight percent (8%) allowed region, and zero percent (0.0%) forbidden region. It complexed with EBJ and CMO-HEM and had 145 amino acids. Both the R-free and R-work values are 0.265 and 0.202, respectively. Ninety-two percent (92.2%) of the destabilized sickle hemoglobin polymer formation (PDB ID: 6DI4) is in the most favorable zone, seven percent (7.6%) is in the allowed region, and zero percent (0.0%) is in the banned region. It complexed with CMO-HEM and has 141 amino acids. The R-work value is 0195 and the R-free value is 0.249.

**2.5 Molecular docking**

PxRy and Biovia Discovery studio software were used to perform molecular docking and binding affinity scores of the optimized ligands and reference medicines against 5E6E, 6BWU, and 6DI4 (Trott and Olson, 2010). Equation 1 was used to determine the ligands' and the standard medications' inhibition constants (Ki) µM. The inhibitory values of a possible active medication should not exceed 10 nM and should fall between 0.1 and 1.0 µM.

$$K_i = e^{\Delta G/RT} \quad (1)$$

where $K_i$ is inhibition constant, ΔG = Binding energy and R = Gas constant.

## 3.0 Results and Discussions

### 3.1similarity screened compounds 5,7-dihydroxy-2-(4-hydroxyphenyl)chromen-4-one.

Ligand-based virtual screening was performed on 5,7-dihydroxy-2-(4-hydroxyphenyl)chromen-4-one (A28) using the SwissSimilarity platform via FP2 fingerprint and pharmacophore screening methods (Zoete et al., 2016)**.** The results obtained from the SwissSimilarity platform identified nine (9) similar compounds CHEMBL293776 (A28-1), CHEMBL371562 (A28-2), CHEMBL1770312 (A28-3), CHEMBL4061417 (A28-4), CHEMBL243664 (A28-5), CHEMBL214321 (A28-6), CHEMBL28 (A28-7), and CHEML463145 (A28-8), as shown in **Table 1 and 2.** CHEML463145 (A28-8) failed ADMET properties and were removed from further analysis.

**Table 1. Similarity screened Compounds from 5,7-dihydroxy-2-(4-hydroxyphenyl)chromen-4-one (A28)**

| | CHEMBL NUMBER | PUBCHEM CID | IUPAC NAMES | SIMILARITY SCORE | |
|---|---|---|---|---|---|
| A28-1 | CHEMBL293776 | 5281628 | 5,7-dihydroxy-2-(4-hydroxyphenyl)-6-methoxychromen-4-one | 0.725 | A28 |
| A28-2 | CHEMBL371562 | 6763 | phenanthrene-9,10-dione | 0.952 | |
| A28-3 | CHEMBL1770312 | 44258296 | 5,7-dihydroxy-2-(5-hydroxy-2,2-dimethylchromen-8-yl)-3-(3-methylbut-2-enyl)chromen-4-one | 0.714 | |
| A28-4 | CHEMBL4061417 | 480802 | 5,7-dihydroxy-2-[4-hydroxy-3-(3-methylbut-2-enyl)phenyl]-6-(3-methylbut-2-enyl)chromen-4-one | 0.784 | |
| A28-5 | CHEMBL243664 | 5280442 | 5,7-dihydroxy-2-(4-methoxyphenyl)chromen-4-one | 0.933 | |
| A28-6 | CHEMBL214321 | 5280666 | 5,7-dihydroxy-2-(4-hydroxy-3-methoxyphenyl)chromen-4-one | 0.712 | |
| FAILED ADMET | CHEML463145 (A28-7) | | | 0.700 | |

**Table 2.** Structures and IUPAC names of similarity compounds from 5,7-dihydroxy-2-(4-hydroxyphenyl)chromen-4-one (A28)

| Code | Structures | IUPAC names |
|---|---|---|
| A28 | 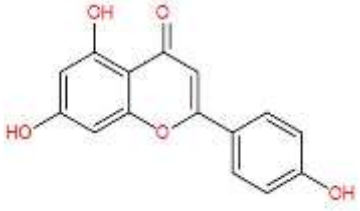 | 5,7-dihydroxy-2-(4-hydroxyphenyl)chromen-4-one |
| A28-1 | 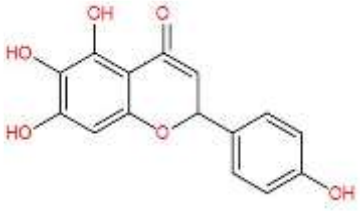 | 5,7-dihydroxy-2-(4-hydroxyphenyl)-6-methoxychromen-4-one |
| A28-2 | 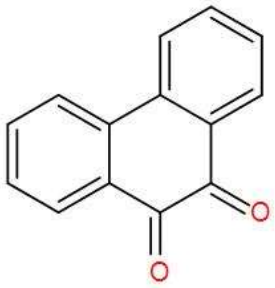 | phenanthrene-9,10-dione |
| A28-3 | 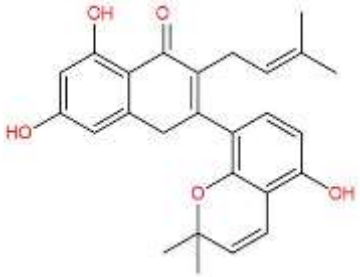 | 5,7-dihydroxy-2-(5-hydroxy-2,2-dimethylchromen-8-yl)-3-(3-methylbut-2-enyl)chromen-4-one |
| A28-4 | 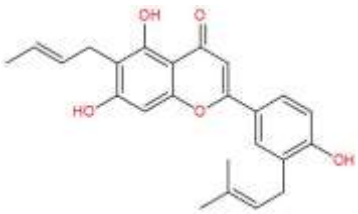 | 5,7-dihydroxy-2-[4-hydroxy-3-(3-methylbut-2-enyl)phenyl]-6-(3-methylbut-2-enyl)chromen-4-one |

| | | |
|---|---|---|
| A28-5 | 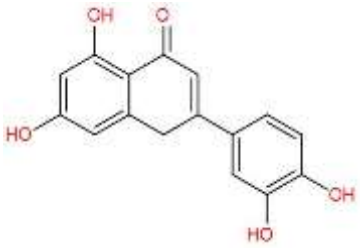 | 5,7-dihydroxy-2-(4-methoxyphenyl)chromen-4-one |
| A28-6 | 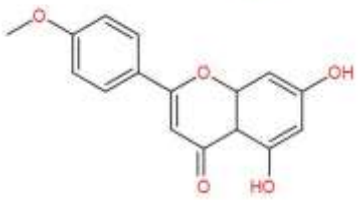 | 5,7-dihydroxy-2-(4-hydroxy-3-methoxyphenyl)chromen-4-one |

### 3.2 Physicochemical and ADMET Properties

The compounds obtained from SwissSimilarity study of 5,7-dihydroxy-2-(4-hydroxyphenyl)chromen-4-one (A28) and the standard drug were subjected to SwissADMET and Pro-Tox II, this was done to compute the physicochemical, ADMET properties of these compounds. The ADMET parameters that were computed include lipophilicity, molecular weight, abbot bioavailability score, blood brain barrier, solubility, and gastrointestinal tract. Table 3 and 4 show the ADME and toxicity results of the compounds respectively. The druglikeness were estimated using Lipinski rule of five which include hydrogen bond acceptor (HBA $\leq$ 10), hydrogen bond donor (HBD $\leq$ 5), molecular weight (150 $\leq$ MW $\geq$ 500), number of rotable bonds (ROBT $\leq$ 10), lipophilicity (LogP $\leq$ 10) (Lipinski, *et al.*, 2004, Veszelka *et al.*, 2018). All the ligands and the drug perfectly obeyed Lipinski rule of five as shown in the Table 3. All ligands had acceptable Topological Polar Surface Area (TPSA) $\leq$ 140 Å$^2$. All the compounds had abbot bioavailability score of 0.5. All had high gastrointestinal tract (GI) which make them suitable drug candidates. Ligands and drug showed no penetrations to blood brain barrier (BBB) and no side effect on the central nervous system (CNS) (Adegbola *et al.*, 2021; Owonikoko *et al.*, 2024). The metabolism shows that A28-5, A28-1, A28-6 and Rivaroxaban displayed non-substrate and inhibitors to CYP3A4, this may lead to overdose of the drug while A28-2, A28-4, and A28-3 has no inhibitory effect on CYP3A4, A28-2, A28-4, A28-3 and rivaroxaban are non- substrate to CYP2D6, A28-4 and A28-1 are non- substrate to CYP2C9.

The prediction class (PC) was used to classify the compounds, Class I and II as fatal if consumed, Class III as toxic if consumed, Class IV as harmful if consumed, Class V perhaps harmful if consumed, Class VI as non- toxic if consumed. A28-2, A28-3, A28-4, A28-5, A28-6, and rivaroxaban had PC to be V, perhaps may be harmful if consumed. A28-1 had PC to be IV and Class IV as harmful if consumed. All the ligands and rivaroxaban displayed inactivity for carcinogenicity and Mutagenicity. All ligands showed activity to immunotoxicity while the ligands displayed inactivity. All had good $LD_{50}$ value except A28-1 with $LD_{50}$ value of 2000 mg/kg indicating that compound may be harmful if swallowed.

**Table 3: ADMET Results for similar compounds obtained from 5,7-dihydroxy-2-(4-hydroxyphenyl)chromen-4-one (A28)**

| L | Druglikness | | | | | | | | Absorption | | | Metabolism | | | | |
|---|---|---|---|---|---|---|---|---|---|---|---|---|---|---|---|---|
| | LogP | W | HBA | HBD | R | TPS | A | L | BB | G | LogS | 1A2 | CI9 | 2C9 | 2D6 | 3A4 |
| **A28-2** | 3.56 | 338 | 5 | 3 | 3 | 90 | 0.5 | 0 | N | H | -6.6 | N | N | Y | N | N |
| **A28-5** | 2.52 | 284 | 5 | 2 | 2 | 79 | 0.5 | 0 | N | H | -4.71 | Y | N | Y | Y | Y |
| **A28-4** | 5.02 | 406 | 5 | 3 | 2 | 79 | 0.5 | 0 | N | H | -2.23 | N | N | N | N | N |
| **A28-1** | 0.22 | 300 | 6 | 3 | 2 | 100 | 0.5 | 0 | N | H | -4.76 | Y | N | N | Y | Y |
| **A28-3** | 2.09 | 420.45 | 6 | 3 | 3 | 100 | 0.5 | 0 | N | H | -7.38 | N | Y | Y | N | N |
| **A28-6** | 0.22 | 300 | 6 | 3 | 2 | 100 | 0.5 | 0 | N | H | -4.87 | Y | N | Y | Y | Y |
| **SD** | 2.95 | 435 | 5 | 1 | 6 | 116 | 0.5 | 0 | N | H | -4.00 | N | Y | Y | N | Y |

G=Gastrointestinal absorption, B=Blood-brain barrier, W=Molecular Weight, A=Abbott Bioavailability, L=Lipinski, R=number of rotatablebond, TPS=Topological polar surface area, HBD= number of hydrogen bond donor, HBA=number of hydrogen bond acceptor LogP= Lipophilicity, LogS=solubility, Y=Yes, N=No.

**Table 4**: **Toxicity studies for the ligands**

| Ligands | TOXICITY | | | | | | |
|---|---|---|---|---|---|---|---|
| | P | C | M | I | H | Cy | $LD_{50}$ |
| **A28-2** | 5 | In | In | A | In | A | 3919 |
| **A28-5** | 5 | In | In | A | A | In | 3200 |
| **A28-4** | 5 | In | In | A | In | In | 3919 |
| **A28-1** | 4 | In | In | A | In | In | 2000 |
| **A28-3** | 5 | In | In | A | In | In | 2500 |
| **A28-6** | 5 | In | In | A | In | In | 4000 |
| **SD** | 5 | In | In | In | In | In | 3200 |

H=Hepatoxicity, C=Carcinogenicity, I=Immunotoxicity, M=Mutagenicity, Cy= Cytotoxocity, PC=Prediction class, Inactive =In, Active =A

### 3.3 Molecular Descriptors of the Ligands

Molecular descriptors were calculated on all six ligands (A28-1, A28-2, A28-3, A28-4, A28-5 and A28-6) and the standard drug Rivaroxaban using density functional theory (DFT) as shown in **Table 3.** These molecular descriptors were electron affinity (EA), ionization potential (IP), HOMO, LUMO, dipole moment (DM), energy band gap, chemical potential, global electrophilicity index, and chemical hardness. A compound's HOMO is its capacity to give electrons away, whereas its LUMO is its capacity to take

them in or take them out. The least reactive and non-polarizable molecule is one with a narrow band gap. The highest occupied molecular orbitals (HOMO) energies were calculated to be -5.81, -6.61, -5.72, -5.74, -5.86, -5.87 and -5.81 eV for the ligands A28-1, A28-2, A28-3, A28-4, A28-5 and A28-6 and the drug, respectively. A28-2 had the highest of HOMO energy than the standard drug indicating that A28-2 has the strongest ability to donate electron to the neighboring compounds or atom and to the target protein. LUMO energies were calculated to be -1.73, -2.99, -1.30, -1.62, -1.70, -1.72, and -1.65 eV for the ligands A28-1, A28-2, A28-3, A28-4, A28-5 and A28-6 and the drug, respectively. The LUMO energy indicated that A28-2 has the strongest ability to accept electron from the target protein, this implies that A28-2 had high inhibition potential with the target than the drug. As shown in Table 3 the dipole moment for the compound and the drug are 3.56, 5.98, 4.45, 3.53, 5.54, 4.33, and 3.94 Debye, respectively. A28-2 would have high chemical reactivity due its highest dipole moment which may hence its binding affinity to the target protein (Yadav *et al*., 2024).

The energy band gaps are 4.08, 3.62, 4.42, 4.12, 4.16, 4.15 and 4.16 eV. A28-3 had the highest value of energy band gaps indicating higher kinetic stability and low reactivity. A28-2 had the lowest energy band gaps value facilitating the transfer of electron and high reactivity. A decrease in chemical hardness corresponds to an increase in reactivity. The values of chemical hardness for the compounds are 2.04, 1.81, 2.21, 2.06, 2.08, 2.08, and 2.08 eV. A28-2 had the lowest value for chemical hardness which implies that it has higher ability to react. Electron affinities are 1.73, 2.99, 1.30, 1.62, 1.70, 1.72 and 1.65 eV. A28-2 had the highest value of EA, indicating that it has the highest capacity to accept electron from other compounds. Global electrophilicity index are -5.62, -8.99, -4.82, -5.38, -5.59, -5.63, and -5.54 eV. The molecular descriptors of the Ligands show A28-2, might have strong interactions with the protein which is also in conformity with the docking results.

**Table 5**: Geometries of Calculated Molecular Description of the Studied Ligands (in vacuum)

| | PUBCHEM CID | H(eV) | L(eV) | DM | Eg(eV) | μ | η | IP | EA | ω | $\Delta\omega^{\mp}$ |
|---|---|---|---|---|---|---|---|---|---|---|---|
| A28-1 | 5281628 | -5.81 | -1.73 | 3.56 | 4.08 | 3.77 | 2.04 | 5.81 | 1.73 | 0.21 | -5.62 |
| A28-2 | 6763 | -6.61 | -2.99 | 5.98 | 3.62 | 4.80 | 1.81 | 6.61 | 2.99 | 0.44 | -8.99 |
| A28-3 | 44258296 | -5.72 | -1.30 | 4.45 | 4.42 | 3.51 | 2.21 | 5.72 | 1.30 | 0.16 | -4.82 |
| A28-4 | 480802 | -5.74 | -1.62 | 3.53 | 4.12 | 3.68 | 2.06 | 5.74 | 1.62 | 0.19 | -5.38 |
| A28-5 | 5280442 | -5.86 | -1.70 | 5.54 | 4.16 | 3.78 | 2.08 | 5.86 | 1.70 | 0.21 | -5.59 |
| A28-6 | 5280666 | -5.87 | -1.72 | 4.33 | 4.15 | 3.80 | 2.08 | 5.87 | 1.72 | 0.21 | -5.63 |

| | | | | | | | | | | | |
|---|---|---|---|---|---|---|---|---|---|---|---|
| Rivaroxaban | 9875401 | -5.81 | -1.65 | 3.94 | 4.16 | 3.73 | 2.08 | 5.81 | 1.65 | 0.34 | -5.54 |

| | PUBCHEM CID | HOMO | LUMO | MEP |
|---|---|---|---|---|
| A28-1 | 5281628 |  | 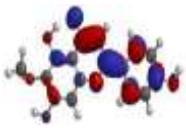 | 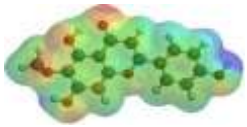 |
| A28-2 | 6763 | 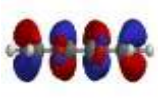 | 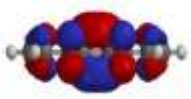 | 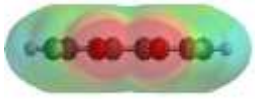 |
| A28-3 | 44258296 | 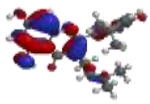 | 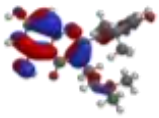 | 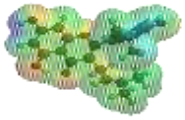 |
| A28-4 | 480802 | 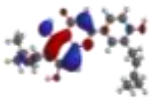 | 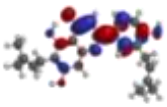 | 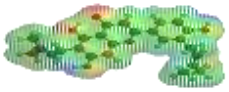 |
| A28-5 | 5280442 | 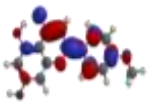 | 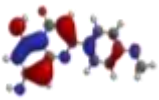 | 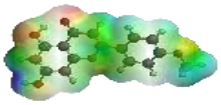 |
| A28-6 | 5280666 | 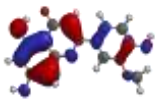 | 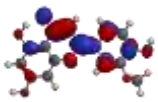 | 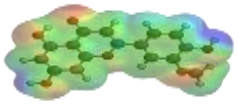 |
| Rivaroxaban | 9875401 |  | 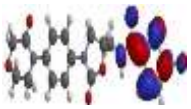 | 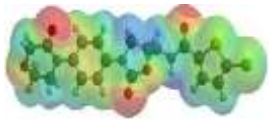 |

**Figure 4:** The frontier orbitals and molecular electrostatic potential (MEP) diagrams for similar compounds and Rivaroxaban (Wavefunction/Spartan 14 version 1.1.4, www.wavefun.

### 3.4 Molecular Docking Results of Similar Ligands from 5,7-dihydroxy-2-(4-hydroxyphenyl)chromen-4-one (A28) with 5E6E

The docking results of the similar ligands with both good ADME and Toxicity test from 5,7-dihydroxy-2-(4-hydroxyphenyl)chromen-4-one (A28) with the target (PDB ID:5E6E) were reported in Table 6. The ligands A28-1, A28-2, A28-3, A28-4, , A28-

5 and A28-6 had -8.6.0, -9.1, -8.1, -9.2, -8.5 and -8.5 kcal/mol, respectively while the standard drugs rivaroxaban had -8.5 kcal/mol binding affinity against the target (PDB ID: 5E6E), with inhibition constant (Ki) of 0.49, 0.25, 1.14, 0.17, 0.59 and 0.59 µM, respectively. A28-2 and A28-4 had higher binding affinities and inhibitory potential for sickle cell diseases than the standard drug. A28-4 interacted with the active site of protein (PDB ID:5E6E) via two (2) conventional Hydrogen bond His 87 and Asn 97, two (2) Pi- Sigma, Val 91, Leu 93, four (4) Pi-Alkyl interactions, Leu 136, Leu 101, Phe 98, and Phe 46 and Tyr 42, Pi-carbon interaction with His 58. Rivaroxaban had two (2) conventional H-bonding His 45 and His 58, one (1) Phe 98 Pi-Sulfur, two (2) Pi-Sigma Leu 91 and Leu 101, one (1) Phe 43 Pi-Pi T-Shaped, five (5) Leu 105, Leu 129, Val 62, Leu 66 and Val 132 Alkyl interactions. The 2D interaction and the surface interactions are shown in the Figure 5.

Table 6: The docking scores, binding affinities, inhibition constant (K*i*), receptor amino acids forming Hydrogen bond and other Electrostatic/ Hydrophobic interaction of optimized ligands and the standard drug with destabilize sickle hemoglobin polymer formation (PDB ID: 5E6E).

| CODE | ΔG(kcal/mol | Ki (µM) | Amino acids forming H bond | Electrostatic/Hydrophobic interactions involved |
|---|---|---|---|---|
| A28-1 | -8.6 | 0.49 | His 58 | Lys 61, Ser 102, Phe 43, Leu 86, His 87, Leu 83, Ala 65, Val 62, Leu 105, Leu 129, Ser 133, Leu 101, Val 132 Leu 66 Leu 136 Phe 98 |
| A28-2 | -9.1 | 0.25 | Nil | His 87, Val 93, Asn 97, Val 62, Leu 101, Leu 136, Val 132, Leu 66, Phe 98, Phe 43, His 58 |
| A28-3 | -8.1 | 1.14 | Nil | Val 96, Leu 100, Phe 36, Pro 37 Thr 38, Thr 39 |
| A28-4 | -9.2 | 0.17 | His 87, Asn 97 | Val 62, Leu 101, Leu 136, Phe 98, Leu 91, Met 32, Tyr 42, Val 93, Phe 43, His 45, Lys 61, Phe 46, Leu 86, His 58 |
| A28-5 | -8.5 | 0.59 | Nil | Leu 129, Ser 102, Ser 133, Leu 105, Val 132, Phe 98, Leu 136, Leu 66, Asn 97, Thr 39, Ala 65, Val 62, Leu 101, Vla 93, His 87, Phe 43, Tyr 42 Met 32 |
| A28-6 | -8.5 | 0.59 | Leu 129 | Val 132, Leu 66, Ala 65, Val 62, Leu 101, Phe 43, His 87, Leu 91, Tyr 42, Asn 97, Thr A39, Met 32, Val 93 Phe 98, Leu 136, Ser 102, Ser 133. |

| | | | | |
|---|---|---|---|---|
| C | -15.7 | $7.1*10^{-6}$ | Nil | Nil |
| R | -8.5 | 0.59 | His 45 and His 58 | Phe 98, Leu 91, Leu 101, Phe 43, Leu 105, Leu 129, Val 62, Leu 66 and Val 132 |

R=Rivaroxaban, C=coligand

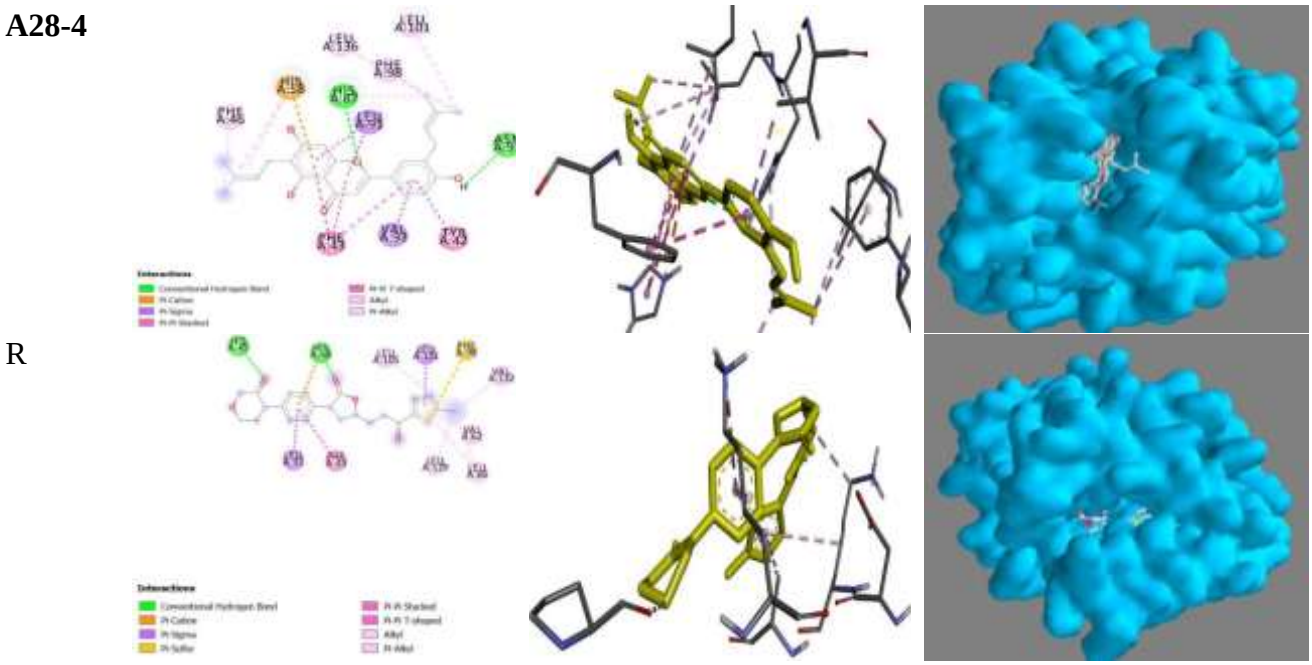


Figure 5: 2D Binding Interactions, Binding Surface A28-4, and rivaroxaban

### 3.5 Molecular Docking of Similar Ligands of 5,7-dihydroxy-2-(4-hydroxyphenyl)chromen-4-one (A28) with ( PDB: 6DI4).

The docking results of the similar ligands with both good ADME and Toxicity test from 5,7-dihydroxy-2-(4-hydroxyphenyl)chromen-4-one (A28) with the target (PDB ID: 6D14) were reported in Table 7. A28-1, A28-2, A28-3, A28-4, A28-5 and A28-6 had -6.9, -7.4, -8.7, -8.2, -8.1 and -7.1 kcal/mol, respectively, while the standard drugs rivaroxaban had -8.0 kcal/mol binding affinity against the target (PDB ID: 6D14), with inhibition constant of 8.7, 3.74, 0.59, 0.96, 1.14, 6.2 and 1.36 µM, respectively. A28-3 had higher binding affinity and inhibitory potential for sickle cell diseases than the standard drug. The implication of this is that compounds A28-3 should be more stable with the target (PDB: 6DI4) and higher inhibitory potential for sickle cell diseases than the standard drugs. A28-3 had conventional hydrogen bond interaction with the protein via Pro 95, Pi-Sigma interaction with Thr 134, A28-4 had Pi-Alkyl interaction via Ala 130 and Pro 72, conventional hydrogen bond interaction with Val 1. Rivaroxaban had four conventional hydrogen bonds with Lys 127, Thr 134, Val 1 and Ser 131, Pi-Alkyl

interaction via Met 76, Pro 77, Leu 2 and Ala 130. The 2D interaction and the surface interactions are shown in the Figure 6.

Table 7: The docking scores, binding affinities, inhibition constant (K*i*), receptor amino acids forming Hydrogen bond and other Electrostatic/ Hydrophobic interaction of optimized ligands and the standard drug with destabilize sickle hemoglobin polymer formation (PDB ID: 6DI4).

| | ΔG(kcal/ mol | Ki (μM) | Amino acids forming H bond with ligands | Electrostatic / Hydrophobic interactions involved |
|---|---|---|---|---|
| A28-1 | -6.9 | 8.7 | Val 1 Thr 134 | Ala 136, Ser 131, Lys 127, Leu 2 |
| A28-2 | -7.4 | 3.74 | Nil | Pro 77, Val 135, Thr 134, Ser 131, Met 76 |
| A28-3 | -8.7 | 0.59 | Pro 95 | Thr 134 |
| A28-4 | -8.2 | 0.96 | Val 1 | Ala 130, Pro 77 |
| A28-5 | -8.1 | 1.14 | Nil | Nil |
| A28-6 | -7.1 | 6.20 | Thr 134 | Ser 131, Pro 77 |
| Coligand | -10.8 | 0.01 | Nil | Nil |
| R | -8.0 | 1.36 | Lys 127, Thr | Met 76, Ala 130, Leu 2, Pro 77 |

L=L-glutamic acid, H=Hydroxurea, R=Rivaroxaban, V=Voxelotor

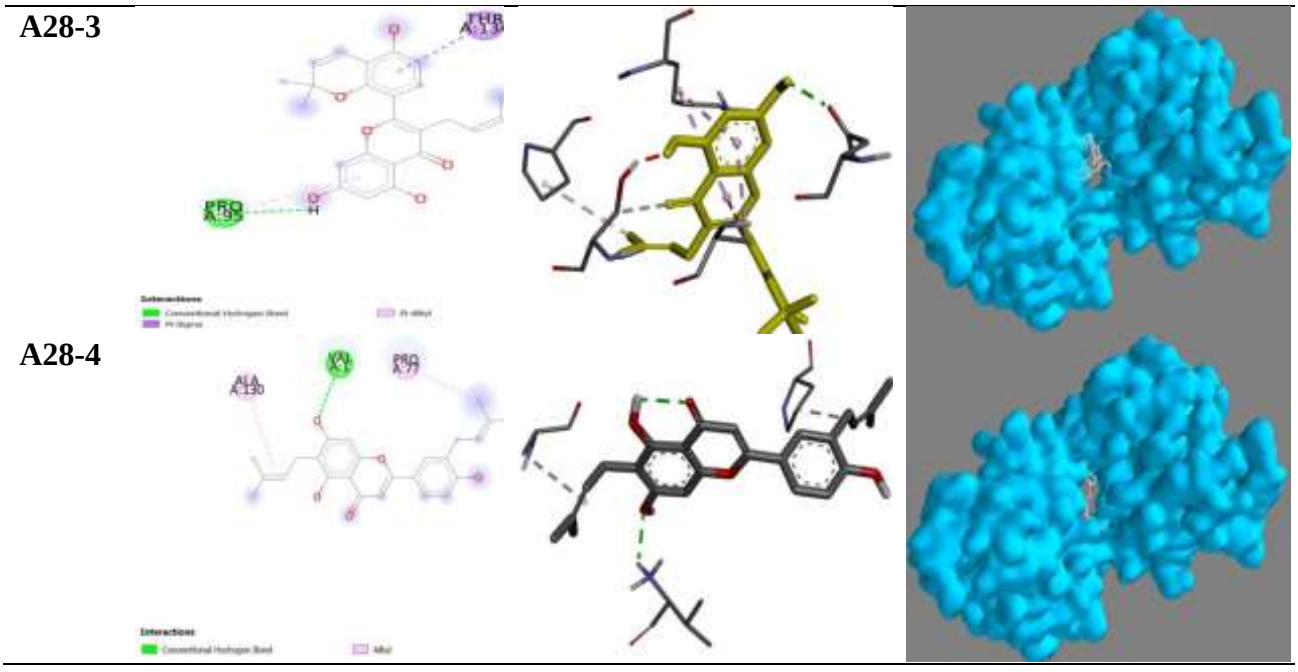

R

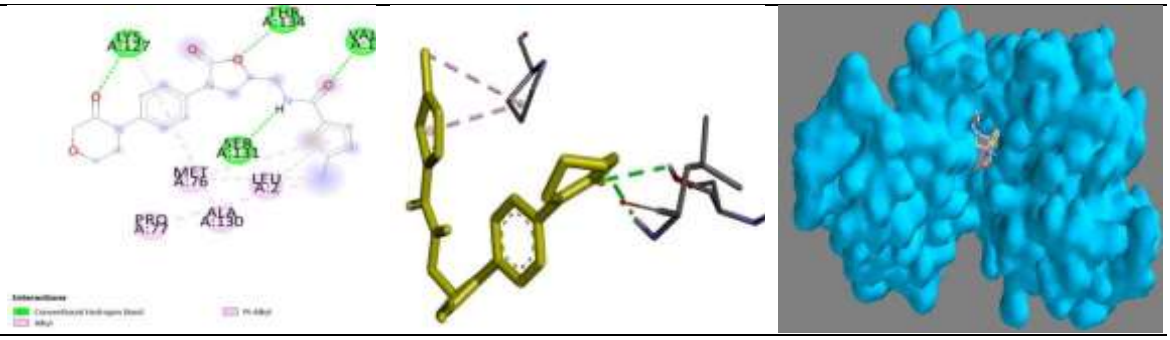

**Figure 6:** 2D Binding Interactions, Binding Surface A28-3, A28-4, and rivaroxaban

### 3.6 Molecular Docking of Similar Ligands of 5,7-dihydroxy-2-(4-hydroxyphenyl)chromen-4-one (A28) with 6BWU.

The molecular docking results of the similar ligands with both good ADME and Toxicity test from 5,7-dihydroxy-2-(4-hydroxyphenyl)chromen-4-one (A28) with the target (PDB ID: 6BWU) were reported in Table 8. The ligands A28-1, A28-2, A28-3, A28-4, A28-5 and A28-6 had -8.7, -9.5, -8.1, -9.9, -8.4 and -8.5 kcal/mol, respectively, while the standard drugs rivaroxaban had -8.1 kcal/mol binding affinities agianst the target (PDB ID: 6D14), with inhibition constant of 0.41, 0.12, 1.14, 0.05, 0.69, 0.59 and 1.14 µM, respectively. A28-3 and A28-4 had higher binding affinities and inhibitory potential for sickle cell diseases than the standard drug.

A28-4 interactions with the target via a conventional hydrogen bond Lys 61, two Pi-Carbon interactions with His 58, His 87, Pi-Pi- Stacked interaction with Phe 43 two Pi-Sigma with Leu 83, Leu 91, Pi-Alkyl with Leu 101, Val 93, Met 32, Tyr 42. Rivaroxaban interacted with target via (1) conventional hydrogen bond with His 87, Pi-Sigma with Phe 43, Amide-Pi Stacked interaction with Lys 61, Pi-Alkyl interaction with Val 62, Ala 65, and Leu 83. The 2D and surface interactions are shown in the Figure 7.

Table 8: The docking scores, binding affinities, inhibition constant (Ki), receptor amino acids forming Hydrogen bond and other Electrostatic/Hydrophobic interaction of optimized ligands and the standard drug with destabilize sickle hemoglobin polymer formation (PDB ID: 6BWU).

| | ΔG(kcal/ mol | Ki (µM) | Amino acids forming H | Electrostatic/ Hydrophobic interactions involved |
|---|---|---|---|---|
| A28-1 | -8.7 | 0.41 | Nil | Leu 86, Leu 101, Leu 105, Leu 66, Leu 136, Val 62, Val 132 Ser 102, Ser 133, Phe 98, His 58 His 87 Lys 61, Ala 65 |
| A28-2 | -9.5 | 0.12 | Nil | Nil |

| | | | | |
|---|---|---|---|---|
| A28-3 | -8.1 | 1.14 | Nil | Lys 99, Val 96, Phe 36, Leu 100, Thy 38, Thr 39, Pro 37 |
| A28-4 | -9.9 | 0.05 | Lys 61 | Leu 83, His 58, His 87, Leu 91, Phe 43, Val 93, Met 32 Leu101, Tyr 42 |
| A28-5 | -8.4 | 0.69 | Ser 102, | Thr 39, Phe 43, Met 32, Asn 97, Phe 98, Leu 66, Val 132, Leu 136, Leu 103, Val 93, Leu 101, His 87 Val 62, Ala 65 |
| A28-6 | -8.5 | 0.59 | Leu 129, Ser 133, | Leu 136, Leu A66, Leu 105, Leu 91, Leu 101, Val 62, Val 132, Ala 65, Ser 102, Asn 97, Met 32, Thr 39, Tyr 42, Phe 43 |
| Coligand | -17.8 | $8*10^{-8}$ | Nil | Nil |
| R | -8.1 | 1.14 | Val 62, His 87 | Ala 65, Leu 91, Val 93, Phe 43, His 58 |

R=Rivaroxaban,

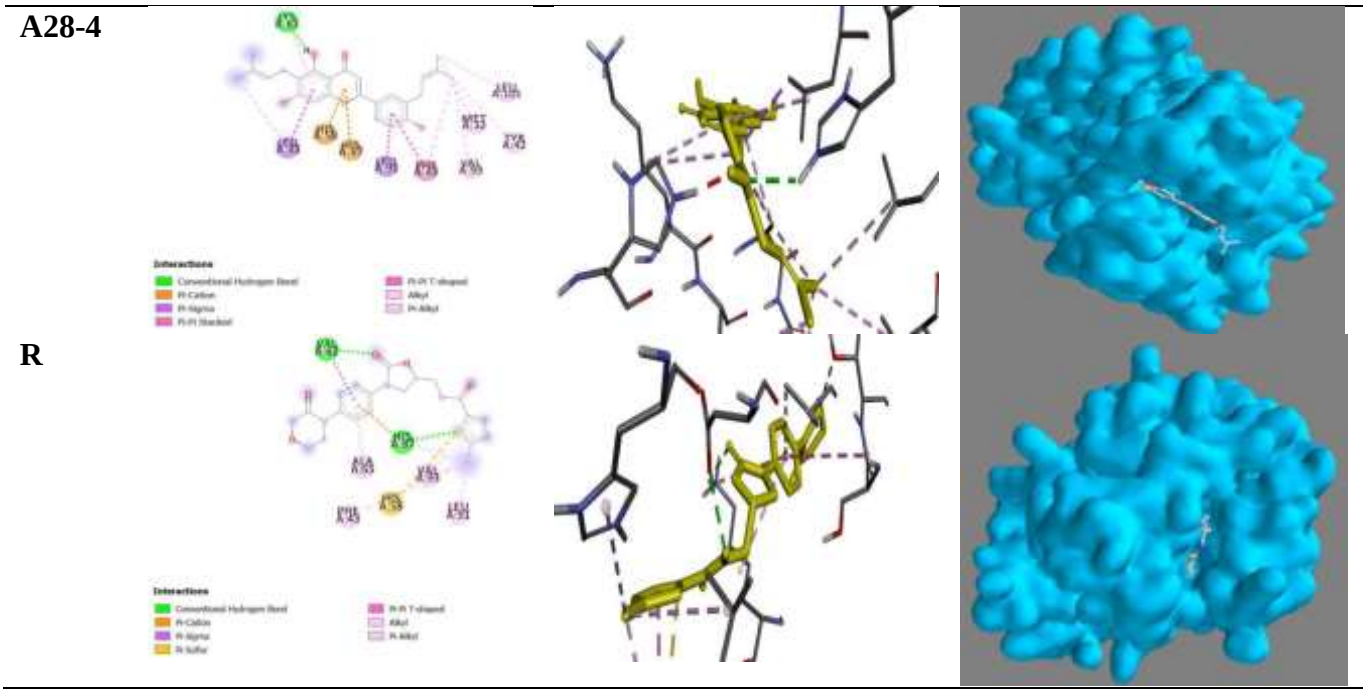


**Figure 7: 2D Binding Interactions, Binding Surface A28-2, A28-4, and rivaroxaban** (Biovia Discovery Studio Visualizer 2021, PyRx-Python Prescription 0.8)**.**

## Conclusion

SwissSimilarity studies of 5,7-dihydroxy-2-(4-hydroxyphenyl)chromen-4-one reveal its potential as a promising therapeutic candidate for combating sickle cell disease. The ADMET and DFT studies revealed that the similar compounds obtained from 5,7-dihydroxy-2-(4hydroxyphenyl)chromen-4-one has future pharmaceutical development and relivance. Molecular docking showed that compounds phenanthrene-9,10-dione (A28-2), 5,7-dihydroxy-2-(5-hydroxy-2,2-dimethylchromen-8-yl)-3-(3-methylbut-2-enyl)chromen-4-one (A28-3), and 5,7-dihydroxy-2-[4-hydroxy-3-(3-methylbut-2-

enyl)phenyl]-6-(3-methylbut-2-enyl)chromen-4-one (A28-4) had stronger binding affinities with the proteins than the standard drug.

**Funding**
No funding received for this work
**Acknowledgments**
The Authors acknowledged the Department of Pure and Applied Chemistry, Ladoke Akintola University of Technology for the computational facilities.

**Availability of Data and Material Statement**: All data generated or analyzed during this study are included in this article.

**Authors contribution**
Yemisi Elizabeth ASIBOR: Conceptualization and writing of original manuscript, Banjo SEMIRE: Supervisor, review, and editing of the manuscript, Abel Kolawole OYEBAMIJI**:** Data curation, Nathaniel Oladoye OLATUNJI**:** Editing, Dayo Felix LATONA: review,

**Conflicts of Interest**
There is no conflict of interest regarding the publication of this article.

**References**

Adegbola, P. I., Semire, B., Fadahunsi, O. S. & Adegoke, A. E. Molecular docking and ADMET studies of Allium cepa, Azadirachta indica and Xylopia aethiopica isolates as potential anti-viral drugs for Covid-19. *Virus Disease* h t t p s : / / d o i . o r g / 1 0 . 1 0 0 7 / s 1 3 3 3 7 - 0 2 1 - 0 0 6 8 2 - 7 (2021).

Adepoju, A.J., Latona, D.F., Olafare, O.G., Oyebamiji, A.K., Abdul-Hammed, M., & Semire, B. Molecular docking and pharmacokinetics studies of *Curcuma longa* (Curcumin) potency against Ebola virus. Ovidius Uni. Ann. Chem. 33(1), 23 - 35, 2022

Asibor, Y. E., Oyebamiji, A. K., Latona, D. F., & Semire, B. **(2024)**. Computational screening of phytochemicals presents in some Nigerian medicinal plants against sickle cell disease. *Scientific Reports*, *14*(1), 26368.https://dio.org/10.1038/s41598-024-75078-w.

Banerjee P, Eskert A, O, Schrey AK Preissner R. ProTox -II: a webserver for the prediction of toxicity of chemicals Nucleic Acids Res. 2018 Jul, 2;46(WI); W257-W263. Doi: 10.1093/nar/gky318. PMID: 29718510 PMCID: PMC6031011.

Becke, A. D. Density-functional thermochemistry. III. The role of exact exchange. *J. Chem. Phys.* **98**, 5648–6565. h t t p s : / / d o i . o r g / 1 0 . 1 0 6 3 / 1 . 4 6 4 9 1 3 (1993).

Bragina, M.E.; Daina, A.; Perez, M.A.S.; Michielin, O.; Zoete, V. The SwissSimilarity **2021** Web Tool: Novel Chemical Libraries and Additional Methods for an Enhanced Ligand-Based Virtual Screening Experience. *Int. J. Mol. Sci.* **2022**, *23*, 811. https://doi.org/10.3390/ ijms23020811.

Daina A, Michielin O, Zoete V. SwissADME: **(2017)** a free web tool to evaluate pharmacokinetics, drug-likeness and medicinal chemistry friendliness of small molecules. Scientific Reports.Mar;7:42717. doi: 10.1038/srep42717.

Jacquemin, D., Perpete, E.A., Ciofini, I., Adamo, C. **(2008)**. Accurate simulation of optical properties in dyes, Accounts of chemical Research ;42:326 – 3344.https://doi.org/10.1021/ar800163d

Laskowski, R. A., & Thornton, J. M. (2022). PDBsum extras: SARS-Cov-2 and AlphaFold models. *Protein science*, *31*(1), 283-289.

Lee, C., Yang, W., Parr, R.G **(1988)**. Development of the Colle-Salvetti correlation-energy formula into a functional of the electron density. Phys. Rev. B 37: 785-

789.https://doi.org/10.1103/PhysRevB.37.785.mainstream. *Clin Transl Med*. 2022;12(4):e766. doi:10.1002/ctm2.766. *Molecules*. 2017;22(2). doi:10.3390/molecules220202.

Lipinski,C.A., Lombardo, F., Dominy, B.W., Feeney P.J., (1997) mainstream. *Clin Transl Med*. **2022;**12(4):e766. doi:10.1002/ctm2.766.

Lipinski, C. A. Lead-and drug-like compounds: The rule-of-five revolution. *Drug Discov. Today: Technol.* **1**(4), 337–343. h t t p s : / / d o i . o r g / 1 0 . 5 7 7 2 / 5 2 6 4 2 (2004).

Middleton, E., Kandaswami, C., & Theoharides, T. C. (2000). The effects of plant flavonoids on mammalian cells: Implications for inflammation, heart disease, and cancer. *Pharmacological Reviews*, *52*(4), 673-751.

Nur, E., Biemond, B. J., Otten, H. E., et al. (2011). Oxidative stress in sickle cell disease; pathophysiology and potential implications for disease management. *American Journal of Hematology*, *86*(6), 484-489.

Owonikoko, A.D., Sodamade A., Olatunde, A.M., Odoje, O.F., & Semire, B. *In silico* Identification of bioactive compounds from *Chasmanthera dependens and Carissa edulis* as potential inhibitors of Carbonic anhydrases (CAs) receptors using a target-based drug design approach. Int. J. Novel Res. Dev. 9(7), b416-b441

Piel, F. B., Steinberg, M. H., & Rees, D. C. (2017). Sickle cell disease. *New England Journal of Medicine*, *376*(16), 1561-1573.

Pérez, L.R.M., Lázaro, J.M., Puentes, N.C., Amador, A. ., Marrugo-Padilla, A. (2024) Identification of proinflammatory pathways and promising bioactive polyphenols for the treatment of sickle cell anemia by in silico study and network pharmacology. Inform Med Unlocked. 49, 101534

Rees, D. C., Williams, T. N., & Gladwin, M. T. (2010). Sickle-cell disease. *The Lancet*, *376*(9757), 2018-2031.

Serjeant, G. R. (2010). The natural history of sickle cell disease. *Cold Spring Harbor Perspectives in Medicine*, *3*(10), a011783.

Shravani S. Pawar, Sachin H. Rohane. Review on Discovery Studio: An important Tool for Molecular Docking. Asian J. Research Chem. 2021; 14(1):86-88. doi: 10.5958/0974-4150.2021.00014.6 Available on: https://www.ajrconline.org/AbstractView.aspx?PID=2021-14-1-14

Tian, Chang Chen, Xue Lei, Jieling Zhao, Jie Liang, CASTp 3.0: computed atlas of surface topography of proteins, *Nucleic Acids Research*, Volume 46, Issue W1, 2 July 2018, Pages W363–W367, https://doi.org/10.1093/nar/gky473.

Trott, O. & Olson, A. J. (2010). AutoDock Vina: Improving the speed and accuracy of docking with a new scoring function, efficient optimization, and multithreading. *J. Comput. Chem.* 31, 455–461. https://doi.org/10.1002/jcc.21334.

Veszelka, S. et al. Comparison of a rat primary cell-based blood-brain barrier model with epithelial and brain endothelial cell lines: Gene expression and drug transport. *Front. Mol. Neurosci.* **11**, 166. https://doi.org/10.3389/fnmol.2018.00166 (2018).

Ware, R. E., de Montalembert, M., Tshilolo, L., & Abboud, M. R. (2017). Sickle cell disease. *The Lancet*, *390*(10091), 311-323.

Yadav, S., Aslam, M., Prajapat, A. *et al.* (2024) Investigate the binding of pesticides with the TLR4 receptor protein found in mammals and zebrafish using molecular docking and molecular dynamics simulations. *Sci Rep* **14**, 24504. https://doi.org/10.1038/s41598-024-75527-6

Zoete, V., Daina, A., Bovigny, C., & Michielin, O. (2016). SwissSimilarity: A web tool for low to ultra-high throughput ligand-based virtual screening. *Journal of Chemical Information and Modeling*, *56*(8), 1399-1404.